Quantum-cascade lasers based on a bound-to-continuum transition

Jérôme Faist,[a] Mattias Beck,[b] and Thierry Aellen
Institute of Physics, University of Neuchâtel, CH-2000 Neuchâtel, Switzerland

Emilio Gini
IQE, Swiss Federal Institute of Technology Zurich, CH-8093 Zurich, Switzerland

A quantum-cascade structure combining the advantages of the three-quantum well and superlattice active regions is demonstrated. In these devices, the emission occurs between a state localized close to the injection barrier and a miniband. A low threshold current density (3.6 kA/cm^2), large slope efficiency (200 mW/A for 35 periods), and peak power (700 mW) are achieved at 30 °C while a peak power of 90 mW is obtained at temperatures as high as 150 °C. © *2001 American Institute of Physics.* [DOI: 10.1063/1.1339843]

The quantum cascade (QC) laser[1] is a unipolar semiconductor laser that has demonstrated pulsed operation at room temperature in the midinfrared wavelength range (3–19 μm). At cryogenic temperatures, good agreement has been obtained between computed and measured threshold current densities and slope efficiencies for a large class of devices,[1,2] In contrast, at 300 K, the predicted value of threshold current density (between 1 and 3 kA/cm^2, depending on whether theoretical or experimental values of the waveguide losses are used) is much lower than the experimental values reported in the literature (between 4.6 and 7 kA/cm^2). Achieving threshold current values closer to the theoretical predictions is crucial to improving the room temperature performances of QC laser devices in order to allow, in particular, continuous wave operation on a Peltier cooler.

In a QC laser, electrons are injected into an upper state (or upper miniband, in the case of superlattice QC lasers[3]) and recombine radiatively to a lower state (or lower miniband). The gain G is proportional to the population inversion Δn between the upper ($n=3$) and lower ($n=2$) states. Let us assume, as shown schematically in Fig. 1, that a fraction η_3 of the current is injected into the upper state, and η_2 into the lower state. In this case, G can be written as

$$G = \sigma \Delta n = \sigma \frac{J}{q_0}\left[\tau_3 \eta_3 \left(1 - \frac{\tau_2}{\tau_{32}}\right) - \eta_2 \tau_2 \right], \qquad (1)$$

where τ_3, τ_2 are the (total) lifetimes, τ_{32} is the intersubband lifetime between the states $n=3$ and $n=2$, and σ is the transition cross section.[1] In the case of a QC, lasers based on a superlattice active region, Eq. (1) can still be applied with the $n=3$ state being the lower state of the upper miniband and the $n=2$ the upper state of the lowest miniband. Equation (1) shows clearly the strong dependence of the gain on both injection efficiencies and the ratio of the lifetimes: one must design a structure which maximizes the difference $\eta_3 \tau_3 - \eta_2 \tau_2$ and minimizes the ratio τ_2/τ_{32}.

High-performance room temperature quantum cascade lasers have so far been demonstrated using two different approaches. The first one is the original design based on a three quantum well (3QW) active region separated from the injection/relaxation region by a tunneling barrier.[1] In the second design, the active region consists of a superlattice, which for the best performances can be ''chirped'' to compensate for the applied field.[3,4] In both cases, the necessity to confine the upper state of the active region requires the laser to be separated into an active region followed by an injection/relaxation region. Although Eq. (1) has limited predictive power because the critical parameters (injection efficiencies and lower state lifetimes) are not easily computed or measured, it qualitatively explains the different strategies these two designs have employed to achieve low-threshold room-temperature performance: the three-quantum well maximizes the first term ($\eta_3 \tau_3$), while the superlattice designs minimize the second term ($\eta_2 \tau_2$). In the 3QW active region devices a large value of η_3 is achieved by the large penetration of the $n=3$ state into the injection barrier[1,5] that enhances the coupling to the $n=3$ state while minimizing the coupling to the lower states of the active region (i.e., $\eta_3 \gg \eta_2$). The extraction of the electrons from the $n=2$ state is enhanced by the resonant nature of the optical phonon transition between the $n=2$ and $n=1$ states,[1] implying a very short value of τ_{21} ($\tau_{21} \approx 0.2$–0.4 ps). However, in such a design, the small value of τ_{21} is misleading because, ultimately, the population of the $n=1$ state (and also $n=2$) is extracted into the injection/relaxation region by a tunneling process. The value of the tunneling time τ_{esc} is difficult to
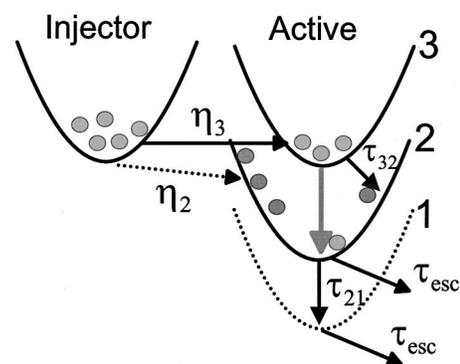

FIG. 1. Schematic description of the relevant levels and injection efficiencies in a cascade laser.

[a]Electronic mail: jerome.faist@unine.ch
[b]Also with Alpes Lasers; electronic mail: www.alpeslasers.com

estimate very accurately. Experimental values obtained in QC structures yield $\tau_{esc} = 2-3$ ps,[6,7] much larger than τ_{21} and the value (0.2 ps) computed assuming the injection region behaves as a continuum. A study using a simple rate-equation approach of the 3QW active region shows that such a slow electron tunneling time, by creating an effective "bottleneck" effect, significantly reduces the population inversion and, therefore, the performance of such a design. This detrimental effect is felt the strongest at high temperatures and high injection currents. In superlattice active region designs, η_2 is made very small by a phase space argument: the $n=2$ state is only one of a manifold of lower states forming the lower miniband and thus injection into this very state is unlikely. Similarly, τ_2 is expected to be very small ($\tau_2 \cong 0.2$ ps) through very efficient intrasubband scattering. In addition, no bottleneck problems are foreseen, since transport in the lower miniband provides a very efficient electron extraction. However, η_3 is not expected to be as large as in the 3QW case since electron injection is not achieved through resonant tunneling.[3]

These considerations are supported by the experimental evidence. Resonant tunneling effects have been observed in the 3QW active region up to room temperature, as expected for large values of η_3.[5,8] The possibility of achieving multi-wavelength operation[9] in superlattice active region designs supports the idea that at least some of the electron injection into the superlattice active region occurs through capture and is therefore less efficient. The high lower state extraction efficiency of superlattice designs is proved by their ability to operate at very high injection current densities (up to 30 kA/cm²).[3]

We propose here a design that attempts to take advantage of the resonant tunneling injection feature of the 3QW design and the electron extraction efficiency of the superlattice design. In this design, shown schematically in Fig. 2, the active region spans the whole period and consists of a chirped superlattice presenting a tilted lower miniband whose width is maximum in the center and decreases on both sides close to the injection barriers. The upper state is created in the first minigap by a small well adjacent to the injection barrier. Its wave function has a maximum close to the injection barrier and decreases smoothly in the active region. This upper state is well-separated from the higher-lying states of the superlattice, lying in its first minigap. It therefore does not need to be confined by separating the structure into an active region and an injection/relaxation region. Because of this large energy separation (60 meV), the injection efficiency η_3 is not reduced by electron injection into higher energy states of the superlattice.[10,11] In addition, this configuration of the wave function should enable an injection efficiency comparable to the one of the 3 QW design.

The structure is grown by molecular beam epitaxy using InGaAs and AlInAs alloys lattice matched on an InP substrate. It consists of a 35 periods active region embedded in an optical waveguide formed on one side by the substrate and on the other by an InP top cladding grown by metalorganic chemical vapor deposition. A good agreement between the electroluminescence spectrum and the computed matrix elements is found, as shown in Fig. 2. Constructive interfer-
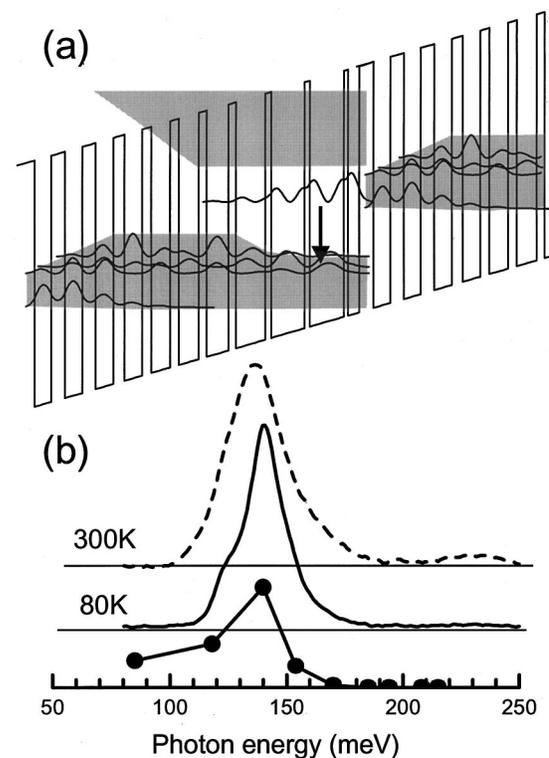

FIG. 2. (a) Schematic conduction band diagram of one stage of the structure under an applied electric field of 3.5×10^4 V/cm. The moduli squared of the relevant wave functions are shown. The layer sequence of one period of structure, in nanometers, left to right and starting from the injection barrier is **4.0**/2.0/**0.7**/6.0/**0.9**/5.9/**1.0**/5.2/**1.3**/3.8/**1.4**/3.5/**1.5**/3.3/**1.6**/3.1/**1.9**/3.1/**2.3**/3.0/**2.4**/2.9 where $In_{0.52}Al_{0.48}As$ layers are in bold, $In_{0.53}Ga_{0.47}As$ in Roman and underlined number correspond to doped layer with Si to $N_d = 3 \times 10^{17}$ cm^{-3}; (b) luminescence spectrum of the active region at 300 and 80 K, as indicated. The applied bias is 9 V. Lower curve: computed oscillator strength of the various transitions from the upper state.

ence effects[12] can be expected to appear in the emission spectra and will be discussed elsewhere.

The devices were mounted junction-side-up onto a copper submount. Figure 3 shows the pulsed (1.5% duty cycle) peak optical power from a single facet versus drive current for various temperatures for a 3 mm long and 28 μm wide device. Knowing the duty cycle, the peak power was ex-
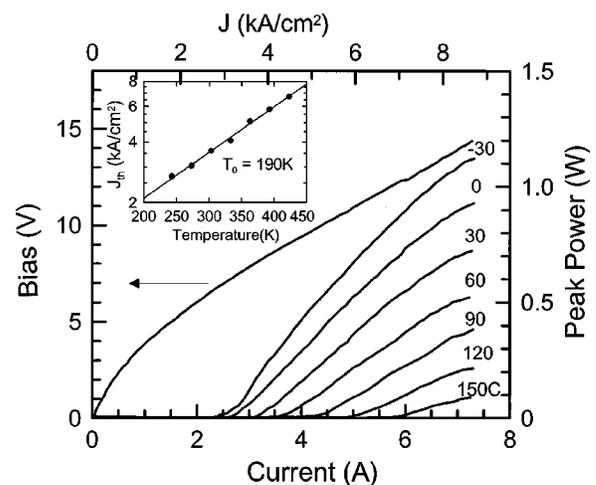

FIG. 3. Peak optical output power vs injected current in pulsed mode at a duty cycle of 1.5% at various temperatures. Inset: Threshold current density as a function of temperature.

trapolated from the measurement of the average power with a thermopile powermeter. The device operates at a wavelength of $\lambda = 9.1\,\mu m$. The slope efficiency is $dP/dI = 200\,mW/A$ at $T = 30\,°C$, with a maximum power of 700 mW at this temperature. Peak powers above 1 W are achieved at $T = -30\,°C$. The small increase in differential resistance at high current could be an indication of a resonant tunneling effect that limits operation with a high injection efficiency to a maximum current density of about 9 kA/cm^2. The high temperature performance is excellent, with a peak power of 90 mW measured at the maximum operation temperature of 150 °C. In the inset of Fig. 3, the threshold current density J_{th} is plotted as a function of temperature. The data between ≈ 270 and 420 K can be described by the usual exponential behavior $J \sim \exp(T/T_0)$ with a value of $T_0 \cong 190\,K$. These devices have been also tested at 30 °C with a 6.5% duty cycle, with a maximum average output power of 25 mW.

[1] J. Faist, F. Capasso, C. Sirtori, D. Sivco, and A. Cho, in *Intersubband Transitions in Quantum Wells: Physics and Device Applications II*, edited by H. Liu and F. Capasso (Academic, New York, 2000), Vol. 66, Chap. 1, pp. 1–83.

[2] C. Gmachl, F. Capasso, A. Tredicucci, D. Sivco, R. Köhler, A. Hutchinson, and A. Cho, IEEE J. Sel. Top. Quantum Electron. **5**, 808 (1999).

[3] F. Capasso, A. Tredicucci, C. Gmachl, D. Sivco, A. Hutchinson, A. Cho, and G. Scamarcio, IEEE J. Sel. Top. Quantum Electron. **5**, 792 (1999).

[4] A. Tredicucci, F. Capasso, C. Gmachl, D. Sivco, A. Hutchinson, and A. Cho, Appl. Phys. Lett. **73**, 2101 (1998).

[5] A. Müller, M. Beck, J. Faist, and U. Oesterle, Appl. Phys. Lett. **75**, 1509 (1999).

[6] J. Faist, F. Capasso, C. Sirtori, D. Sivco, A. Hutchinson, M. Hybertsen, and A. Cho, Phys. Rev. Lett. **76**, 411 (1996).

[7] S. Blaser, L. Diehl, M. Beck, J. Faist, U. Oesterle, J. Xu, S. Barbieri, and F. Beltram (unpublished).

[8] C. Sirtori, F. Capasso, J. Faist, A. Hutchinson, D. Sivco, and A. Cho, IEEE J. Quantum Electron. **34**, 1722 (1998).

[9] A. Tredicucci, C. Gmachl, F. Capasso, D. Sivco, A. Hutchinson, and A. Cho, Nature (London) **396**, 350 (1998).

[10] M. Troccoli, G. Scamarcio, V. Spagnolo, A. Tredicucci, C. Gmachl, F. Capasso, D. Sivco, A. Cho, and M. Striccoli, Appl. Phys. Lett. **77**, 1088 (2000).

[11] P. Kruck, H. Page, C. Sirtori, S. Barbieri, M. Stellmacher, and J. Nagle, Appl. Phys. Lett. **76**, 3340 (2000).

[12] J. Faist, F. Capasso, C. Sirtori, K. West, and L. Pfeiffer, Nature (London) **390**, 589 (1997).